Subsurface zone detected in pure nickel by positron annihilation; Hall-Patch effect notification

Jerzy Dryzek

Institute of Nuclear Physics Polish Academy of Sciences, PL-31342 Kraków, Poland
Corresponding author: jerzy.dryzek@ifj.edu.pl

ABSTRACT

A dry sliding test and sequential etching technique, combined with positron lifetime measurements on pure nickel, revealed an area of damage below the worn surface extending to a depth of hundreds of micrometers. Some correlation was found between the value of the mean positron lifetime measured directly on the worn surface and the coefficient of friction. The obtained dependency rather confirms the normal Hall-Patch regime. There was no correlation with the specific wear rate.

Keywords: Nickel, Positron lifetime spectroscopy, Subsurface zone, Dry sliding test

1. Introduction

Sliding contact between bare metals results in a frictional force, and surface damage characterized by the coefficient of friction (CoF) and wear rate. Additionally, microstructure changes under worn surfaces (WS) occur as well. They are extended quite deep from this surface which is why this zone is called the subsurface zone (SZ). The origin of the changes is not only plastic deformation, i.e., nucleation and motion of dislocations but also other processes. One of them and well documented is dynamic recrystallization (DRX), which seems to play a key role in the generation of refinement grains in the area adjacent to the WS [1], [2], [3]. This is reflected also in the layered structure of the SZ, [4]. Directly beneath the WS, a tribolayer with very fine, randomly oriented grains is located, some authors report on nanocrystalline or ultra-nanocrystalline grains even with sizes smaller than 20 nm [6], [7]. This layer can be up to 10 μm thick. Beneath, another layer with thin and elongated parallel to the WS grains is observed [4], [5]. This is believed to be the result of the geometric DRX process [3]. Much deeper is the plastically deformed region with large initial grains, full of atomic-scale defects, including dislocations. Such a layered microstructure is confirmed by both the SEM, and EBSD methods, and also by the positron annihilation methods [5].

It can be noted that in the literature, the tribolayer has been labeled also: the WS, a layer usually containing the counterface material as a result of mechanical mixing of the ultrafine-grained material, and any oxide induced both by the sliding [8]. This layer is similar to the formation elements in the ball milling scenario, which is why it is sometimes called a mixed layer. Additionally, this is a thin layer of about 1 μm thickness as in copper, see Fig. 2 in Ref. [9]. The authors simplify the description of the SZ which according to them consists of a tribolayer and below extensive plastic deformation layer located just on the base material. This is a rather crude approximation.

Many authors have tried and still tried to link the microstructure of grain refining in the tribolayer with the frictional properties of metals [10], [11], [12], [13]. According to Bowden and Tabor, the CoF is roughly expressed as the ratio of shear strength to hardness, both of which depend on the properties of the metal, which change upon plastic deformation and the appearance of grain refinement. The latter is interesting because, according to the Hall-Petch relationship, smaller grain size increases the uniaxial yield strength and induces an increased ductility of the metals. This is still dislocation-mediated plasticity but grain boundaries (GBs), in this case, act as an obstacle to nucleating and propagating dislocations. This is the normal Hall-Petch regime. However, when the grain structure is extremely refined, grain size is less than 10 nm, and there exists a sufficiently large density of interconnected grain boundaries, GBs sliding prevails [14]. The properties of GBs exhibit many features in common with glass-forming liquids, as results from molecular dynamic simulations [15]. Thus, when the volume fraction of GBs is sufficiently high, the polycrystalline material begins to exhibit viscoelastic properties, additionally strongly dependent on temperature, which has a large impact on the plastic deformation of these materials. The authors call this the inverse Hall-Petch regime because the shear strength decreases and as a result, the CoF value may also decrease. This mechanism may have

potential application in the reduction of the CoF value widely discussed in the literature, see Ref.[16].

It is well known that GBs especially high angle GBs (HAGBs) contain open volume defects, such as clusters of vacancies, which can be easily detected by the positron lifetime measurement. In short, they significantly increase the lifetime of positrons trapped in them. Reducing the grain size results in an additional increase in the mean positron lifetime as a greater fraction of the positrons can reach HAGBs, which is well described theoretically and experimentally in the so-called positron diffusion trapping model, see Appendix or Ref. [17], [18]. Thus, one can try to relate friction properties to the positron lifetime value. This can be instructive because friction itself is realized at the macro scale, while positrons monitor properties at the atomic scale.

Normally, the transition between the normal and the inverse Hall-Petch regime, as a decrease in the CoF value, is observed at a very small load of several tens of mN under special conditions, vacuum, etc. Then, the produced tribolayer with fine grains is very thin, about 100 nm [12]. In typical applications, much larger loads of several N are used, and the conditions are not complicated. It seems that positron annihilation technique can provide new information on Hall-Petch regimes and their influence on tribological properties in such cases.

In principle, positron technique allow us to observe defects either in very thin films nanometer thick, located on the surface, or in the much deeper region of more than 1-2 µm and more. The first requires to use of a special technique called slow positron beam, however, the latter conventional technique is enough. The first use of the slow positron beam in the friction application means that pure gold exposed to the dry sliding does not show any significant changes at the WS [19] indicating an amorphous, highly damaged or mixed layer. However the application of the sequential etching (SET) technique with the measurement of conventional ^{22}Na positrons has revealed many interesting features that result in many other papers, see [20] and [21]. It is therefore reasonable to use this technique to study the Hall-Petch effect in tribolayer studies.

The studies are carried out on pure nickel subjected to a dry sliding test (ST). Nickel is a face-centered cubic metal for which the crossovers have been theoretically predicted [22]. Positron lifetime measurements in SET are used to detect the SZ below the WS and show its properties. The resulting microstructure and wear rate and CoF measurements are analyzed to find possible correlations.

2. Experimental details

2.1 Preparation of samples

In our studies, we used nickel of purity of 99.5 % purchased from Goodfellow. In positron studies of SZ, sample preparation is crucial. In our experiments, samples had the form of a disc with a diameter of 10 mm and a thickness of 2 mm. The base surfaces of each disk were grinded and polished. To remove defects from the manufacturing process, all discs were annealed at 1150 °C in a vacuum of 10^{-5} Torr for 1 h and then slowly cooled with the furnace. The measurement of the positron lifetime spectrum for such prepared samples revealed only a single lifetime component equal to 105.9 ± 0.3 ps and this corresponds with a bulk value reported in the literature, i.e., 105 ps [23], 110 ps [10], 108 ps [25], [26]. The theoretical value calculated using the LMTO method with BN and GGA parameterizations by Campillo Robles et al. is about 108 ps [27]. Thus, all the damage and defects after the ST will be generated by the ST only.

2.2 Sliding test

The ST has been performed in severe conditions and equipment has been described in previous publications, see Ref. [4]. Briefly, this is a disk-on-disk experiment in air, so the base surface of the virgin sample disk, fixed on the load arm is pressed with a normal load against the rotating surface of the disk made of high-speed steel, HS18-0-1 with a microhardness HV as 8000 MPa. The applied loads were equal to 20, 50, 100, and 150 N, which corresponds to the estimated pressures of 0.25, 0.64, 1.3, and 1.9 MPa. The speed of the disk to the sample was about 37 cm/s. The sample and disk surfaces were cleaned with acetone before the ST. No oxidation on the surfaces was noticed after. However, the thin film of the possible oxide layers does not affect the energetic positrons they pass through and annihilate in the interior of the sample.

2.3 The CoF and wear rate measurement

At this time a force transducer placed in the load arm recorded the tangentional force over a track distance of 0.2 m over the whole sliding distance. The accuracy of the tangentional force measurement was about 0.012 N. The ratio of tangential to normal load is the coefficient of friction (CoF).

During ST the mass of the sample, as a result of wear is reduced continuously. After a certain sliding distance, monitoring the change of the sample mass using the laboratory scales allows us to determine the dependency of the loss of mass as the function of sliding distance. This is a linear relationship, in which the slope is divided by the density, to obtain the wear volume, of the sample and the applied load gives the value of the specific wear rate in the unit of m^3/Nm. The mass was measured with an accuracy of 10^{-4} g.

2.4 Positron lifetime measurements

Digital spectrometer APV–8702 (purchased from TechnoAP) with two detectors based on the BaF_2 scintillator and H3378-50 photomultiplier (purchased from Hamamatsu) has been used in the measurement of all positron lifetime spectra. Each of the spectra contained about 10^6 counts and was resolved for two lifetime components τ_1

τ_2 with the corresponding intensities I_1 and I_2, respectively. These quantities are sensitive to the presence of open volume defects being traps for positrons. Obtaining them one can calculate the mean positron lifetime as follows $\bar{\tau} = \tau_1 I_1 + \tau_2 I_2$,

this is a robust parameter that is also sensitive to defects that localize positrons giving contribution in the measured spectrum. The LT-polymer program was used to analyze all the measured spectra, [28].

2.5 Depth profiling technique

Changes in the microstructure caused by the ST in the virgin sample were detected using the SET, i.e. measurement of the positron lifetime spectrum followed by etching a surface layer of a certain thickness of about a few micrometers. This procedure is carried out until a bulk value of the positron lifetime is obtained. This is a destructive technique but can detect microstructure changes down to hundreds of micrometers deep. A nitric acid solution was used for etching, and the thickness of the sample before and after etching was measured with a digital micro-screw with an accuracy of ±1 μm. The depth from WS is defined as half the thickness difference between the thickness of the sample after the ST and after etching.

2.6 Microhardness measurements

The Zeiss optical, a reflected light microscope, Neophot 21, (OM) was used to observe the surface of the sample and perform the Vickers microhardness (HV) measurements. In this case, the applied load in an indentation was equal to 40 g. The average from seven indentations was used for the calculation of HV.

3. Results and discussion

3.1 Dry sliding results

The measured depth profile of the $\overline{\tau}$ value for virgin nickel samples subjected to the ST with various loads is shown in Fig. 1. It can be seen that the highest value is directly on the WS, then decreases to the bulk value, marked by the horizontal straight line. This line helps determine the total range of the SZ. For a load of 20 and 50 N, it is about 250 and 500 μm respectively, for a load of 100 N and 150 N it is probably well above 1 mm, and the measurement was stopped at a depth of 400 μm. This is the first time such a large range has been observed compared to our previous studies for different metals. Typically, the SZ range was much shorter, e.g. in a similar metal, i.e. iron, for a load of 50 N, the total range was only 150 μm [29]. Another interesting feature, in this case, is the linear decrease of the $\overline{\tau}$ value as a function of depth, which is marked with solid straight lines in Fig.1. In our previous studies, an exponential decay relationship, or more generally a sigmoidal relationship was observed, [29], [30]. For the highest loads of 100 and 150 N, a rapid increase in the $\overline{\tau}$ values is observed at a depth of less than 20 μm, see an inset in Fig. 1. A local minimum can also be observed at a depth of approximately 40 μm.

Individual values of components: τ_1 and τ_2 and their intensities, the resolved from the lifetime spectra, vs. depth are demonstrated only for the load of 100 N, see Fig. 2. (For other loads the dependencies are similar and will be not presented.) The values of τ_1 range from 170 to bulk values,
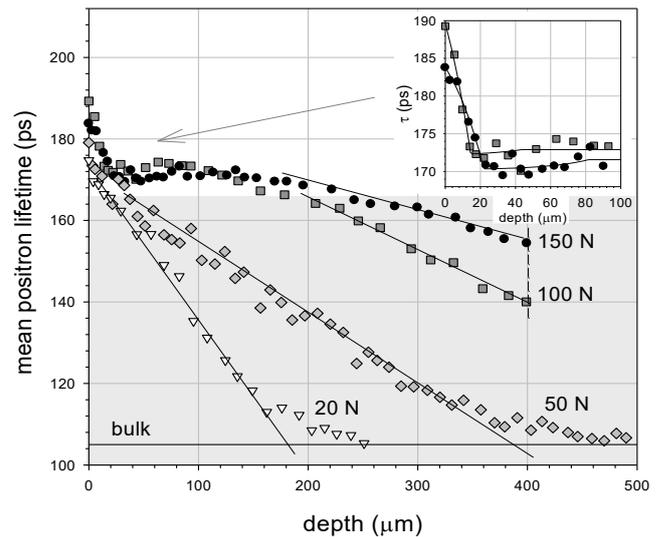
Fig. 1 The depth dependence of the mean positron lifetime, $\overline{\tau}$ obtained for the virgin nickel samples subjected to the ST: The sliding distance was 25 m and the applied loads were ranged from 20 to 150 N. The straight horizontal line represents the bulk positron lifetime value measured for the virgin sample before the ST. The gray region, marked below 166 ps represents the area where the plastic deformation takes place. Straight lines are drawn by the eye. In the inset, the local minimum near the WS is shown in detail.

i.e., 105 ps (closed circles in Fig. 2 b whereas the τ_2 value ranges from 340 to 180 ps. The positron lifetime in a monovacany in nickel is equal to 180 ps, [27], values less than this one indicate the positron trapping at jogs at dislocation lines or loops, or monovacancies places near dislocation. For instance, the positron lifetime trapped at a single vacancy on the edge dislocation according to the theoretical calculations is equal to 164 ps, [10]. So this component is associated with dislocations, of which a great number is generated during plastic deformation [24]. Values larger than this one point out the positron trapping at the vacancy cluster, whose size is larger when the lifetime value is larger. For instance, the lifetime of 192 ps corresponds to divacancy, but more than 300 ps can be more than ten vacancies in a cluster [10]. The clusters can result from the coalescence of mono vacancies, but they are also present at HAGB's. From Fig. 2 c one can deduce that at a depth less than 20 μm such a large cluster is present, they are responsible for the sudden increase of the $\overline{\tau}$ value seen in Fig. 2 a, and in Fig. 1. This is the region of refinement grains, which size is less than 300 nm, as deduced from our former studies, e.g., for iron [5]. They are randomly oriented, which suggests that their source is a continuous DRX process. Many authors tagged such a process near WS [1], [31], [32]. Thus a significant increase in the τ_2 value points out the small grains, their size is comparable or less with positron diffusion length. This enables the localization of positrons in grain boundary defects.

The region between 20 and about 40 μm is of interest. In this region, the τ_2 value decreases from about 340 to about 220 ps, while the intensity increases from 10% to about 40%,
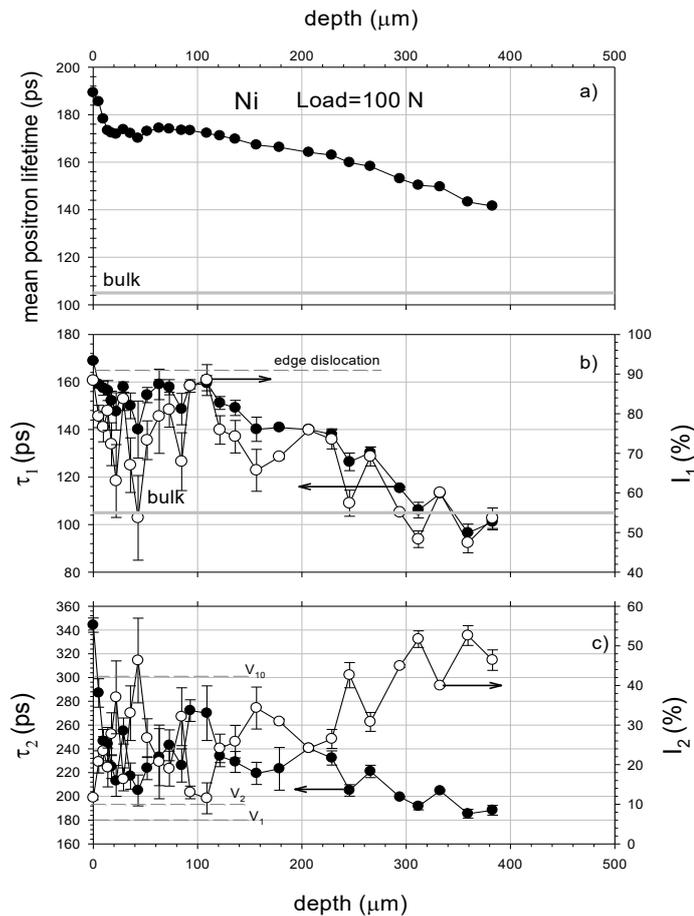
Fig. 2 The depth dependence of the mean positron lifetime, $\bar{\tau}$ (a), positron lifetime components τ_1 (b), and τ_2 (c) (closed circles) values, and their intensities (open circles) (right axis) obtained for the pure virgin nickel sample subjected to the ST: The sliding distance was 25 m and an applied load was equal to 100 N. The gray horizontal line in (a) and (b) represents the bulk positron lifetime value measured for the virgin sample before the ST. The calculated positron lifetime for edge dislocation, monovacancy vacancy V_1, and vacancy cluster which consists of two and ten vacancies V_2 and V_{10} are shown by horizontal dashed gray lines.

Fig. 2 c. This region also is marked in Fig. 1 a in an inset, as a visible local minimum, where, according to previous studies, it indicated that geometric DRX is taking place [5]. The grains are long and very thin, and some texture is observed. When the grains have sufficient internal stress, which is easy to obtain near the WS, the grains are "pinched off" and form new grain-free ones that have essentially no internal stress. It seems that such strain relaxation is reflected in a local decrease in the apparent the $\bar{\tau}$ value. However, also in this layer, new grains may be formed from DRX. The high temperature in the asperities regions caused by sliding contact can initiate the nucleation of new grains, but a large deformation quickly stops their growth, [33], [34]. This process as in the case of geometric DRX generates randomly oriented grains. Above the depth of 60 µm, a continuous decrease in the $\bar{\tau}$ value is observed, mainly due to the decrease in the dislocation component and its intensity (open circles) in Fig. 2 b. Cluster size decreases as the τ_2 value

decreases gradually. In Fig. 1, it can be seen that for the load of 20 N and 50 N, no local minimum is observed. For a load of 20 N, the $\bar{\tau}$ value decreases almost linearly with increasing depth, and similarly for a load of 50 N. However, in both cases, the τ_2 value on the WS did not increase significantly, for 20 N it was 260 ps, and for 50 N it was 275 ps, Fig. 2 c. Thus, it can be argued that at a small load, the tribolayer and the layer with elongated grain do not occur or are so thin that they are not detected by positrons, as at the load of 100 or 150 N in our experiment.

3.2 Compression test

Comparing the results obtained in the ST with similar ones, but when a virgin nickel has been subjected to a uniaxial compression test, it can help identify the region of the SZ where only plastic deformation is acting in the sliding test. The results of the compression test are shown in Fig. 3. As the thickness reduction (or shear strain) increases, the $\bar{\tau}$ value increases and saturates at about 165 ps when the strain is greater than 15% Fig. 3 a. This is due to the increase in the dislocation component, Fig. 3 b. The τ_2 value also saturates at around 240 ps, Fig. 3 c (closed circles). The intensities of the lifetime components (open circles) are not significantly different. Comparing Fig. 3 with Fig. 2 or Fig. 1, it can be concluded that typical plastic deformation in the ST can occur only at greater depths than WS. The gray region marked in Fig. 1, with the $\bar{\tau}$ value less than 166 ps, represents this region. For example, for a load of 100 N, plastic deformation occurs mainly at a depth greater than 200 µm, below this depth, there must be another mechanism of defect formation. This can undoubtedly be DRX, continuous, and geometric, it can generate very small grains, which are indicated by the large value of the $\bar{\tau}$ and τ_2 value.

3.3 The CoF measurement

Along with the ST of the virgin samples, CoF and specific wear rate were also monitored. Fig. 4 a shows the results. After a short distance of about 5 m, the CoF value reaches the steady-state values. Measurements of the SZ defect depth profile, shown in Fig. 1 and 2 were made in this state, i.e. after a sliding distance of 25 m. Surprisingly, the value of CoF depends on the applied load. It is characteristic that for the lowest loads, the CoF value is low and amounts to about 0.3, while at higher loads it increases to about 0.4. Comparing Fig. 4 and 1, it can be concluded that a low CoF value corresponds to the case when the tribolayer is not well developed and/or visible in the positron results.

It can be argued that in this case there is still a layer of native oxides on the surface, which allows for easy sliding. It seems that such a film acts as a lubricant. Indeed, the use of lubricants in the ST as above causes a significant change in the generated SZ as was observed for copper, see Fig. 8 in Ref. [35] and recently in vanadium [36]. As the applied load increases, this layer is removed and a strong adhesion appears associated with pure metallic interfaces. This causes an increase in the CoF value.
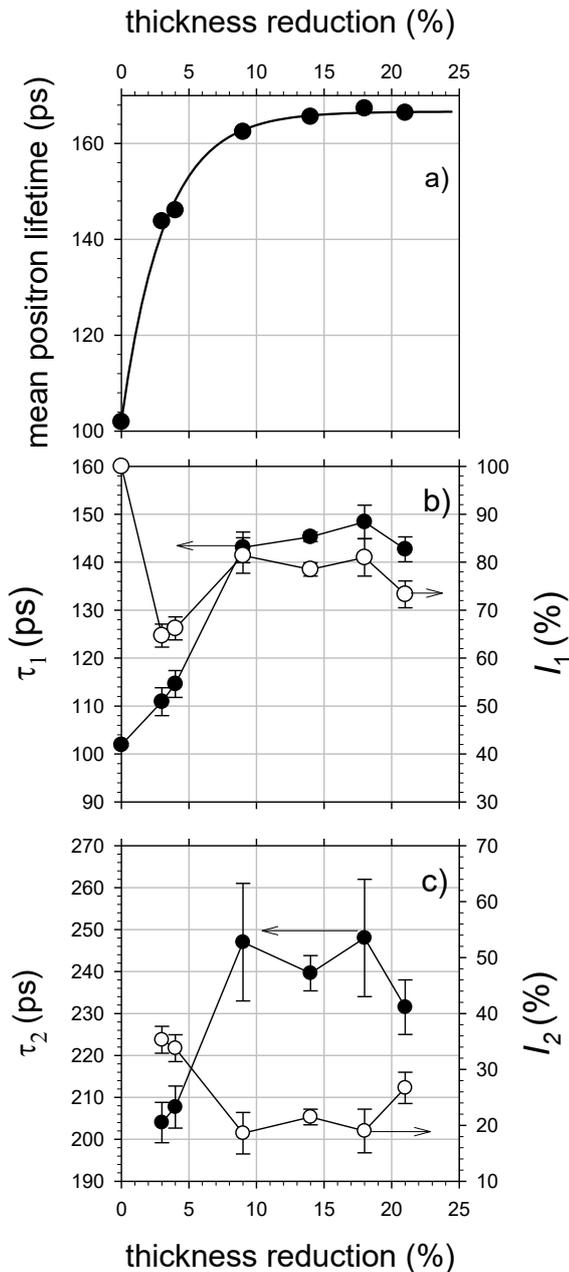
Fig. 3 The values of the mean positron lifetime $\overline{\tau}$ (a), the first, τ_1, (b) and the second, τ_2, (c) lifetime component, (closed circles), and their intensities, I_1 (c) and I_2 (d), (open circles) as the function of the thickness reduction of the compress deformed sample. The solid line in (a) represents the best fit by the following equation: $\overline{\tau} = \tau_{sat} + (\tau_{bulk} - \tau_{sat})\exp(-c\,\varepsilon)$, where the values of adjustable parameters are equal to τ_{sat}=166.6±1 ps, c=0.314±0.020, and τ_{bulk}=102.1±1.7 ps. ε represents the thickness reduction in %.

However, one can notice also a weak correlation between the CoF and the $\overline{\tau}$ values on the WS, (the square of the correlation coefficient of about 0.62,) solid straight line in Fig. 4 b. (Keep in mind that CoF is a very macroscopic feature,

while positron lifetimes are atomic-scale properties, so a perfect match cannot be expected.) Thus, it can be argued that the appearance of a well-developed tribolayer with refinement grains causes an increase in the CoF value. This confirms a case of the normal Hall-Patch regime, finer grains, here marked with an increase in the $\overline{\tau}$ and τ_2 values, cause an increase in the shear strength of nickel, and thus an increase in the CoF value. The inverse Hall-Patch regime should be associated rather with decreases in the CoF value with the increase of this positron annihilation characteristic values. This was not observed in these studies.

Nevertheless, according to Bowden and Tabor's theory of inelastic adhesive, CoF also depends inversely on the hardness or yield strength. The increase in microhardness near WS is well documented in the literature. This is due to hardening, i.e. the accumulation of dislocations and other defects that impede plastic deformation. The Vickers microhardness measured for the virgin nickel sample is equal to about (730.5±6) MPa, while after the ST the microhardness on the worn surface increases significantly to (2081.2±36) MPa. Thus, this effect also occurs in nickel.

While a week correlation was observed between the $\overline{\tau}$ and CoF values, no such correlation was observed for the measured specific wear rate, dashed line in Fig. 4 b (open circles). The square of the correlation coefficient obtained in this dependency is about 0.062. It could have seemed that the specific wear rate should be much more sensitive to microstructure changes in the SZ than CoF. But that is not the case.

4. Closing remark

The results obtained for nickel do not indicate that a simple correlation between SZ features wear rate and CoF can be unequivocally determined. However, authors who have linked the CoF values with fine grain structure also had difficulties. They had to measure the CoF value first, then prepare the sample, take a cross-section perpendicular to the WS, and then prepare that surface for transmission electron microscopy images. This is a complicated procedure that can obscure the final results, which can be read in the conclusions: *Formation of stable ultrafine nanocrystalline layers with 2 to 10 nm size grains underneath the wear surface **may be responsible** for the observed friction transitions, **possibly due** to transition from traditional dislocation plasticity to deformation controlled by grain boundaries,* Ref. [12]. No direct correlation between grain size and CoF value is hard to find in Ref. [16] too. Positron measurements are much simpler as they are performed directly on the WS where the CoF was previously determined. For that reason, they are recommended for such studies in the future.

Conclusions

As with other metals exposed to ST in nickel, a well-defined SZ is generated, but for the first time, such a large
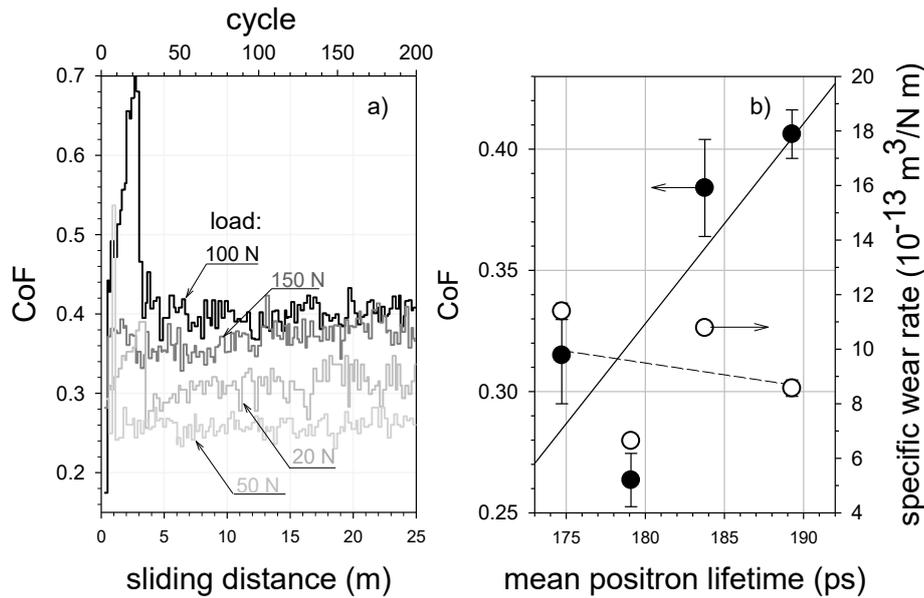
Fig. 4 CoF values recorded as the function of sliding distance for different loads (a). CoF values after a sliding distance of 25 m correlated with the values $\bar{\tau}$ measured at the WS (b) (closed circles). The values of the specific wear rate (b) are represented by open circles. The straight solid and dashed lines are the least square fit to the experimental points closed circles and open circles, respectively.

total range of this zone of approximately several hundred micrometers depending on the applied load has been observed. For example, for a load of 50 N, this range is about 0.5 mm. Near the WS the trybolayer, which is characterized by a rapid increase in the $\bar{\tau}$ value is detected. Its thickness is about 20 μm. This layer contains dislocations but also clusters which consist of about ten vacancies, that may be associated with HAGB's of refinement grains generated in DRX process. Below this layer, the next layer is extended up to 60 μm where smaller clusters, mainly divacancies are observed. This layer is characterized by the existence of a local minimum in the $\bar{\tau}$ values, which may be associated with strain relaxation. However, for the first time, it was shown the increase o in the $\bar{\tau}$ values at the WS was correlated with the increase in the CoF value. This suggests a normal Hall-Patch regime, which means no effect of GBs on friction. At the same time, no correlation with a specific wear rate was observed.

Compliance with Ethical Standards

The author declares that they have no known competing financial interests or personal relationships that could have appeared to influence the work reported in this paper.

Appendix

The base of the positron diffusion trapping model is based on the following assumptions, see Fig. (A1):

(i) the implanted positrons after thermalization are randomly and uniformly distributed in the spherical grain of radius R,

(ii) they randomly walk (diffuse) in the grain and can also reach the grain boundary.

(iii) the annihilation rates of positrons inside the grain are

equal to λ_g and are trapped at GB λ_{GB}.

(iv) the trapping rate at the GB is infinity.

The solution of the diffusion equation allows us to derive the following equation for the mean positron lifetime:

$$\bar{\tau} = \tau_g + 3(\tau_{GB} - \tau_g)\frac{L_+}{R}\left[\coth\left(\frac{R}{L_+}\right) - \frac{L_+}{R}\right], \qquad A(1)$$

where L_+ is the positron diffusion length in the grain, $\tau_g = 1/\lambda_g$, and $\tau_{GB} = 1/\lambda_{GB}$.
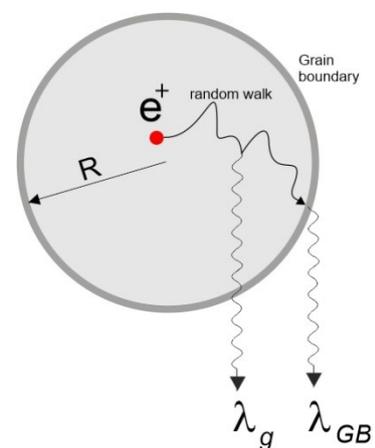
Fig. A1 Scheme of the diffusion trapping model. A positron can annihilate in the spherical grain of radius R with the annihilation rate λ_g and from the trapped state at the GB with the annihilation rate λ_{GB}. Inside grain, a positron randomly walks and can reach the GB in this process.

Literature

[1] D. A Rigney,. L. H Chen,. M. G. S Naylor, A. R Rosenfield, Wear Processes in Sliding Systems, Wear 100 (1984) 195-219. https://doi.org/10.1016/0043-1648(84)90013-9

[2] T. Sakai, A. Belyakov, R. Kaibyshev, H. Miura, J. J.Jonas, Dynamic and post-dynamic recrystallization under hot, cold and severe plastic deformation conditions, Progress in Materials Science 60, (2014) 130-207. https://doi.org/10.1016/j.pmatsci.2013.09.002

[3] K. Huang, R. E. Logé, A Review of Dynamic Recrystallization Phenomena in Metallic Materials, Materials and Design 11 (2016) 548-574. https://doi.org/10.1016/j.matdes.2016.09.012

[4] J. Dryzek, M. Wróbel, Detection of tribolayer in pure iron using positron annihilation and EBSD techniques, Tribology International 144 (2020) 106133-9. https://doi.org/10.1016/j.triboint.2019.106133

[5] J. Dryzek, M. Wróbel, Detection of dynamical recrystallization in a tribolayer of pure molybdenum using positron annihilation and EBSD techniques, Wear, 466-467 (2021) 203524-13. https://doi.org/10.1016/j.wear.2020.203524

[6] A.M. El-Sherik, U. Erb, G. Palumbo, K.T. Aust, Deviations from hall-petch behavior in as-prepared nanocrystalline nickel, Scripta Mater. 27 (1992) 1185-1188. https://doi.org/10.1016/0956-716X(92)90596-7

[7] K.S. Kumar, H. Van Swygenhoven, S. Suresh, Mechanical behavior of nanocrystalline metals and alloys, Acta Mater. 51 (2003) 5743-5774. https://doi.org/10.1016/j.actamat.2003.08.032

[8] R. L. Deuis; C. Subramanian, J. M. Yellup, Dry sliding wear of aluminum composites-a review, Composites Science and Technology 57 (1997) 415-435. https://doi.org/10.1016/S0266-3538(96)00167-4

[9] D. A. Rigney, Some thoughts on sliding wear, Wear 152 (1992) 187-192.

https://doi.org/10.1016/0043-1648(92)90214-S

[10] E. Kuramoto, H. Abe, M. Takenaka, F. Hori, Y. Kamimura, M. Kimura, K. Ueno, Positron annihilation lifetime study of irradiated and deformed Fe and N, J. Nucl. Mat. 239 (1996) 54-60.

https://doi.org/10.1016/S0022-3115(96)00432-1

[11] A.G. Frøseth, P.M. Derlet, H. Van Swygenhoven, Dislocations emitted from nanocrystalline grain boundaries: nucleation and splitting distance, Acta Mater. 52 (2004) 5863-5870.

https://doi.org/10.1016/j.actamat.2004.09.001

[12] S.V. Prasad, C.C. Battaile, P.G. Kotula, Friction transitions in nanocrystalline nickel, Scripta Materials 64 (2011) 729-732. https://doi.org/10.1016/j.scriptamat.2010.12.027

[13] M. Chandross, J. F. Curry, T. F. Babuska, P. Lu, T. A. Furnish, A. B. Kustas, B. L. Nation, W. L. Staats, N. Argibay, Shear-induced softening of nanocrystalline metal interfaces at cryogenic temperatures, Scripta Materialia 143 (2018) 54-58. https://doi.org/10.1016/j.scriptamat.2017.09.006

[14] M. Chandross, N. Argibay, Ultimate strength of metals, Physical Review Letters 124 (2020) 125501-5. https://doi.org/10.1103/PhysRevLett.124.125501

[15] H. Zhang, D. J. Srolovitz, J. F. Douglas, J. A. Warren, Grain boundaries exhibit the dynamics of glass-forming liquids. Proc. Natl. Acad. Sci. USA 106, 7735-7740 (2009). https://doi. org/ 10. 1073/ pnas. 09002 27106 https://doi.org/10.1073/pnas.0900227106

[16] M. Chandross, N. Argibay, Friction of metals: a review of microstructural evolution and nanoscale phenomena in shearing contacts, Tribol. Lett. ,69 (2021) 119-27. https://doi.org/10.1007/s11249-021-01477-z

[17] J. Dryzek, A. Czapla, E. Kusior, Positron annihilation studies of the multilayer Cu-Cu3Sn system, J.Phys. Condens. Matter 10 (1998) 10827-10838. https://doi.org/10.1088/0953-8984/10/48/006

[18] R. Würschum, L. Resch, and G. Klinser, Phys. Rev. B 97, 224108 (2018). https://doi.org/10.1103/PhysRevB.97.224108

[19] J. Dryzek, E. Dryzek, B. Cleff, Study of subsurface zones induced by friction and wear using positron annihilation method, Applied Surface Science, 116 (1997) 236-240. https://doi.org/10.1016/S0169-4332(96)01061-6

[20] J.Dryzek, E. Dryzek, T.Stegemann, B.Cleff, "Positron Annihilation Studies of Subsurface Zones in Copper", Tribology Letters, 3 (1997) 269. https://doi.org/10.1023/A:1019141424218

[21] J. Dryzek, "Positron profilometry. Probing materials depths for enhanced understanding", (SpringerBriefs in Materials 2023). https://doi.org/10.1007/978-3-031-41093-2

[22] A. R. Hinkle, J. F. Curry, H. Lim, B. L. Nation, M. R. Jones, J. Wellington-Johnson, P. Lu, N. Argibay, M. Chandross, Low friction in bcc metals via grain boundary sliding, Physical Review Mater 4 (2020) 063602-9. https://doi.org/10.1103/PhysRevMaterials.4.063602

[23] H.-E. Schaefer, Investigation of Thermal Equilibrium Vacancies in Metals by Positron Annihilation, phys. stat. sol. (a) 102 (1987) 47-65. https://doi.org/10.1002/pssa.2211020104

[24] L. C. Smedskjaer, M. Manninen, M. J. Fluss, An alternative interpretation of positron annihilation in dislocations, J. Phys. F 10 (1980) 2237-49. https://doi.org/10.1088/0305-4608/10/10/019

[25] R. Würschum, W. Greiner, R. Z. Valiev, M. Rapp, W. Sigle, O. Schneeweiss, H.-E. Schaefer, Interfacial free volumes in ultra-fine grained metals prepared by severe plastic deformation, by spark erosion, or by crystallization of amorphous alloys, Scr. Metal Mater. 25 (1991) 2451-2456. https://doi.org/10.1016/0956-716X(91)90048-6

[26] J. Cižek, I. Prochazka, M. Cieslar, I. Stulikova, F. Chmelik, R. K. Islamgaliev, Positron-lifetime investigation of thermal stability of ultra-fine grained nickel, phys. stat. sol. (a) 191 (2002) 391-408. https://doi.org/10.1002/1521-396X(200206)191:2<391::AID-PSSA391>3.0.CO;2-H

[27] J. M. Campillo Robles, E. Ogando, F. J. Plazaola, Positron lifetime calculation for the elements of the periodic table, J. Phys. Condens. Matter 19 (2007) 176222(20pp). https://doi.org/10.1088/0953-8984/19/17/176222

[28] J. Kansy, LT programs. Available at: http://prac.us.edu.pl/~kansy/index.php?id=ltpolym. Accessed date: 16 November 2010

[29] J. Dryzek, Positron studies of subsurface zone in pure iron induced by sliding, Tribol. Lett. 42 (2011) 9-15. https://doi.org/10.1007/s11249-010-9742-x

[30] J. Dryzek, Temperature studies of the subsurface zone in pure titanium exposed to a dry sliding test , Proc. IMechE Part J: J. Eng. Tribol. 236 (2021) 1962-1971. https://doi.org/10.1177/13506501211060591

[31] J.R. Timothy, C.A. Schuh, Sliding wear of nanocrystalline Ni-W: Structural evolution and the apparent breakdown of Archard scaling, Acta Materialia. 58 (2010) 4137-4148. https://doi.org/10.1016/j.actamat.2010.04.005

[32] B. Yao, Z. Han, K. Lu, Correlation between wear resistance and subsurface recrystallization structure in copper, Wear 294 - 295 (2012) 438-445. https://doi.org/10.1016/j.wear.2012.07.008

[33] M. Scherge, D. Shakhvorostov, K. Pöhlmann, Fundamental wear mechanism of metals, Wear 255 (2003) 395-400. DOI:10.1016/S0043-1648(03)00273-4 https://doi.org/10.1016/S0043-1648(03)00273-4

[34] J. Dryzek, A. Kozłowska, Recrystallization in subsurface zone seen by positron annihilation. Tribology International, 43 (2010) 447-454. https://doi.org/10.1016/j.triboint.2009.07.009

[35] J. Dryzek, M. Wróbel, Evolution and thermal stability of the subsurface zone in copper formed in dry and lubricated sliding tests studied by positron annihilation and EBSD techniques, Wear, 486-487 (2021) 204077-12. https://doi.org/10.1016/j.wear.2021.204077

[36] J. Dryzek, M. Wróbel, Positron annihilation and EBSD studies of subsurface zone created during friction in vanadium, J. Tribol., 145 (2023) 071703-10. https://doi.org/10.1115/1.4062297